Arabian Journal of Chemistry (2022) **15**, 104153

King Saud University

Arabian Journal of Chemistry

www.ksu.edu.sa
www.sciencedirect.com

ORIGINAL ARTICLE

The effects of biologically important divalent and trivalent metal cations on the cyclization step of dopamine autoxidation reaction: A quantum chemical study

Nejc Umek

Institute of Anatomy, Faculty of Medicine, University of Ljubljana, Korytkova ulica 2, 1000 Ljubljana, Slovenia

Received 6 March 2022; accepted 22 July 2022
Available online 27 July 2022

KEYWORDS

Dopamine;
Autoxidation;
Metal cations;
Neurodegeneration;
Parkinsonism

Abstract Dopamine is the most essential monoaminergic neurotransmitter involved in the pathophysiology of neurodegenerative disorders, and its autoxidation has been recognized as one of the potential trigger factors for dopaminergic neuron loss. The cyclization of dopamine *o*-quinone was shown to be the irreversible and rate-limiting step of the autoxidation reaction at physiologic pH values. Furthermore, various metal ions such as Al^{3+}, Fe^{3+}, Fe^{2+}, Co^{2+}, Ni^{2+}, Cu^{2+}, Zn^{2+}, Cd^{2+}, Pb^{2+}, and Mn^{2+} have been clinically associated with neurodegeneration, especially Parkinsonism and dementia. It has been proposed that these metal ions could increase the rate of the dopamine autoxidation reaction; however, the exact mechanism has not yet been fully understood. Using advanced quantum chemical calculations with the inclusion of solvent effects we showed that except for Mn^{2+}, the studied metal cations could form complexes with dopamine *o*-quinone and significantly increase the dopamine *o*-quinone cyclization rate in aqueous solution; first, by enabling the cyclization to proceed spontaneously without the attack of the unprotonated amino group by hydroxide ion; second, by decreasing the intrinsic activation energy; and third, by decreasing the free energy of protonated amino group deprotonation. The latter also decreases the protective effect of acidic pH on dopamine autoxidation found in synaptic vesicles. The results are fully consistent with experimental data and provide deeper understanding of the effects of metal cations on the dopamine autoxidation reaction at physiologic pH values.

E-mail address: nejc.umek@mf.uni-lj.si

Peer review under responsibility of King Saud University.

Production and hosting by Elsevier

https://doi.org/10.1016/j.arabjc.2022.104153

1. Introduction

Dopamine is the most essential monoaminergic neurotransmitter involved in the pathophysiology of neurodegenerative disorders such as Parkinson's disease, Alzheimer's disease, and dementia with Lewy bodies (Martorana and Koch, 2014; Pavlin et al., 2016; Piggott et al., 1999). While several advances have been made in understanding the molecular pathophysiology of these neurodegenerative diseases, the trigger factor for the monoaminergic neuron loss characteristic of the disorders remains poorly understood. A recent focus of interest in an attempt to illuminate this blind spot is the non-enzymatic autoxidation reaction of dopamine in an aqueous solution (Segura-Aguilar et al., 1998). This autoxidation reaction chain involves an initial oxidation step that yields the catecholamine quinone form and superoxide anion, subsequent decomposition of the superoxide anion into various reactive oxygen species (ROS), and cyclization of the quinone form with intramolecular Michael addition (Baez et al., 1994). The product of the cyclization step is aminochrome, a neuromelanin precursor which has been implicated in a broad range of pathophysiological mechanisms underlying neurodegenerative disorders. In one-electron reduction by flavoenzymes that use NADH or NADPH as electron donors the aminochrome can be transformed into leukoaminochrome *o*-semiquinone radical. The latter is very reactive with oxygen and can deplete both NADH and oxygen required for ATP synthesis. Moreover, aminochrome can also form adducts with different proteins causing protein degradation dysfunction, α-synuclein aggregation, and promoting oxidative stress and neuroinflammation (Paris et al., 2010; Segura-Aguilar, 2019). Other biochemical processes, for example, the mitochondrial electron transfer chain and degradation of biogenic amines by monoamine oxidase (MAO) are besides catecholamine autoxidation also important sources of ROS in the central nervous system (Cassagnes et al., 2018; Pavlin et al., 2016). All the above processes may induce focal neurodegeneration of dopaminergic neurons and contribute to Parkinson's disease and other neurodegenerative disorders (Herrera et al., 2017).

The cyclization step of the catecholaminergic autoxidation reaction has been recognized as the irreversible and rate-limiting step across a broad pH range (Bacil et al., 2020; Bindoli et al., 1999; El-Ayaan et al., 1998; Lin et al., 2017; Schindler and Bechtold, 2019). Using quantum chemical calculations, we recently proposed a reaction mechanism of autoxidation of dopamine and other catecholamines explaining the complex pH dependence of their autoxidation rate at a broad pH range (Umek, 2020; Umek et al., 2018) and demonstrated that low pH values are critical to maintain dopamine stability and prevent its autoxidation. Moreover, we showed that protonation and introduction of positive charge to quinone group of catecholamine *o*-quinones in aqueous solution could change the mechanism of the cyclization step and its kinetics by significantly increasing the rate of the reaction (Umek, 2020).

Various metal ions have been associated with neurodegeneration, especially Parkinsonism and dementia. For example, exposure to manganese (Mn), copper (Cu), and cadmium (Cd) has been clinically associated with psychiatric symptoms and extrapyramidal motor dysfunction typical of Parkinsonism. Moreover, the iron (Fe) concentrations in the substantia nigra correlate well with the motor dysfunction symptoms in Parkinson's diseases (Paris and Segura-Aguilar, 2011). Lead (Pb) and nickel (Ni) can cause cognitive deficiencies, tiredness, lethargy, ataxia, and behavioural disorders (Canfield et al., 2003; Lamtai et al., 2018). Furthermore, zinc (Zn), cadmium (Cd), and aluminium (Al) accumulation has been associated with neural damage and Alzheimer's disease (Branca et al., 2018; Morris and Levenson, 2017; Wang et al., 2018); and high levels of cobalt (Co) can cause tinnitus, deafness, vertigo, visual changes, optic atrophy, tremor and peripheral neuropathy (Catalani et al., 2012). Although metal neurotoxicity has been extensively investigated, the exact molecular mechanisms of toxicity are not sufficiently understood due to broad interactions of metal ions with synaptic transmission and synaptic plasticity at the presynaptic, synaptic, and postsynaptic levels (Sadiq et al., 2012).

Several divalent and trivalent metal cations such as Fe^{3+}, Mn^{2+}, Cu^{2+}, Co^{2+}, Zn^{2+}, Al^{3+}, Ni^{2+}, Pb^{2+} have been found to interact with the phenolic group of catecholamines and forming organometallic complexes in aqueous solution (Gergely et al., 1981; Grgas-Kužnar et al., 1974; Harrison et al., 1968; Jameson and Neillie, 1966, 1965; Lloyd, 1995; Martin, 1994). Moreover, it has been reported that in the central neural system, iron and dopamine coexist in the dopaminergic vesicles (Ortega et al., 2007). Oxidizing metal cations catalyse dopamine autoxidation in aerobic and anaerobic conditions by direct oxidation of dopamine to semiquinone, and by oxidizing the latter to *o*-quinone which is the form that subsequently undergoes the irreversible cyclization and forms aminochromone (Paris and Segura-Aguilar, 2011; Salomäki et al., 2018). Such oxidation of dopamine to dopamine *o*-quinone by metal ions shows inverse pH dependence increasing the rate at acidic pH and decreasing the rate at alkaline pH (Salomäki et al., 2018). On the other hand, the cyclization step is also highly pH-dependent, and its rate significantly decreases at acidic and neutral pH, where it becomes the rate-limiting step of dopamine autoxidation, and increases at alkaline pH where oxidation of dopamine to quinone form becomes rate-limiting (Bacil et al., 2020; Lin et al., 2017; Salomäki et al., 2018; Umek et al., 2018). Therefore, in physiological conditions where dopamine is mainly located in synaptic vesicles with the acidic environment (pH of ~5.6) and in the cytosol and extracellular fluid with pH of ~7.1 and ~7.4, respectively, the cyclization step represents the most important rate-limiting step of autoxidation reaction (Chaudhry et al., 2008; Du et al., 2014; Mani and Ryan, 2009; Pregeljc et al., 2020). Although the effects of various metal ions on the autoxidation of dopamine and other catecholamines have been extensively studied, their effect on the cyclization step of autoxidation remains poorly understood (Sun et al., 2018). Accordingly, the present study aimed to elucidate the effects of different divalent and trivalent metal cations that have been clinically associated with neurotoxicity on cyclization step of dopamine autoxidation reaction in aqueous solution at physiological pH range using advanced quantum chemical methods with the inclusion of solvent effects.

2. Materials and methods

2.1. Quantum chemical calculations

Gaussian 16 software package (Frisch et al., 2016) was used to perform all the quantum chemical calculations to study the organometallic complexes of metal cations and dopamine *o*-quinone, and to determine the effect of metallic cations on the reaction mechanism of dopamine *o*-quinone cyclization step. The initial structures of dopamine *o*-quinone and dopamine *o*-quinone complexed with various metallic cations were built using the Molden v5.9 software package (Schaftenaar and Noordik, 2000). To decrease computational cost, a 1:1 M ratio of metal cation to dopamine *o*-quinone was considered for all studied complexes. All the structures were optimised at the M06/Def2-TZVPP level of theory because M06 functional and Def2-TZVPP basis set are recommended for organometallic chemistry and for noncovalent interactions (Weigend and Ahlrichs, 2005; Zhao and Truhlar, 2008). Solvent effects were considered by the universal solvation model, based on density (SMD) (Marenich et al., 2009), which is a solvent reaction field model that describes the solute as a composite of interlocking spheres and the solvent as a dielectric continuum. A dielectric constant of water ($\varepsilon = 78.3$) was applied to represent an aqueous solution. While studying reaction kinetics, the same procedure was applied to optimize geometries of products after cyclization. The transition state search started from the manually set initial geometries.

Analysis of harmonic vibrational frequencies was performed for all stationary points. Calculated frequencies were used for thermodynamic corrections of relative free energies at 298.15 K. The reactant and product minima have only real frequencies, while the transition states have one imaginary frequency and visualisation of its eigenvector corresponds to the reactive motion. Atomic charges were calculated by the Merz–Singh–Kollman scheme. For metal atoms, the corresponding universal force field radii scaled by 1/1.2 were applied (Rappé et al., 1992). Frontier molecular orbital analysis was performed at the same level of theory and the solvation model to assess the chemical reactivity of studied complexes. Where applicable, high-spin (HS), intermediate-spin (IS), and low-spin (LS) states were considered. Described quantum chemical methods with the inclusion of solvent effect represent an established tool for studying binding and reactivity and can provide important knowledge and insight into properties of otherwise unattainable systems (Dalla Torre et al., 2019; Khan et al., 2018; Kržan et al., 2020).

2.2. Electron density analysis

To perform a topological analysis of the electron density between metal cations and dopamine *o*-quinone, we used a quantum theory of atoms in molecules (QTAIM) (Bader, 1991) that provides critical points of the electron density and the atomic boundaries. The bond critical points (BCPs) are saddle points of the electron density between two bonded atoms and provide information about the nature of bonding. Small electron density values, charge depletion, and positive energy densities are characteristic for van der Waals, ionic and hydrogen bonds, and metal–metal interactions, while large electron densities, charge concentration, and negative energy densities are characteristic for covalent interactions. The topological parameters at the BCPs were calculated using the multiWFN3.1 software package (Lu and Chen, 2012) on the previously optimized structures. Wavefunction files derived by Gaussian 16 at M06/Def2-TZVPP/SMD level of theory served as input files.

2.3. Calculation of pKa values

The pKa values of organometallic complexes of metal cations and dopamine *o*-quinone were calculated using the thermodynamic cycle shown in Fig. 1 (Liptak et al., 2002). If acid donates a proton to bulk water, there is an analytical relation between the free energy for the process, acid dissociation constant (K_a), and pH value of water (Bronsted, 1928). For the deprotonation reaction

$$AH^+_{aq} = A_{aq} + H^+_{aq} \tag{1}$$

and

$$pKa = -logK_a \tag{2}$$

$$\Delta G_{aq} = -2.303RTlogK_a \tag{3}$$

the pKa is given by

$$pKa = \frac{\Delta G_{aq}}{2.303RT} \tag{4}$$

where ΔG_{aq} is the Gibbs energy of deprotonation in an aqueous solution, R is the gas constant, and T is the absolute temperature.

For the thermodynamic cycle used

$$\Delta G_{aq} = \Delta G_{gas} + \Delta\Delta G_{sol} \tag{5}$$

$$\Delta\Delta G_{sol} = \Delta G_s(H^+) + \Delta G_s(A) - \Delta G_s(AH^+) \tag{6}$$

For calculations of gas-phase reaction energies and solvation free energies (ΔG_s) the M06/Def2-TZVPP level of theory and SMD reaction field model were used. The latter was chosen because it was found to be the most accurate in predicting catecholamine *o*-quinone pKa values (Umek, 2020). The solvation free energy of a proton $\Delta G_s(H^+) = -264.0$ kcal mol^{-1} and the gas phase standard free energy of a proton $G_{gas}(H^+) = -6.287$ kcal mol^{-1} at 298.15 K were adopted from the literature (Ho and Coote, 2009; Liptak et al., 2002). Please note, that value of $G_{gas}(H^+)$ includes reaction free energy of hydronium ion formation and is hydration free energy. For conversion of ΔG_{gas}, for which the 1 atm reference state is used for calculation, to 1 M reference state, which is used for ΔG_s calculation, the following equation was used:

$$\Delta G_{gas}(1M) = \Delta G_{gas}(1atm) + RTln(24.46) \tag{7}$$

The pKa values were therefore calculated using the equation:

$$pKa = \frac{G_{gas}(A) - G_{gas}(AH^+) + \Delta G_s(A) - \Delta G_s(AH^+) - 268.39}{1.365} \tag{8}$$

The latter equation was derived by combining Eqs. (4)–(7) and experimental values for $\Delta G_s(H^+)$ and $G_{gas}(H^+)$.

Free energy differences of proton transfer from the ionizable group with a certain pKa value to bulk water with a certain pH value were calculated using the equation:

$$\Delta G = k_B T \ln(10)(pKa - pH) \tag{9}$$

It is worth stressing that pKa calculations are extremely demanding since deprotonation is equivalent to SN1 reaction (Perdan-Pirkmajer et al., 2010; Sham et al., 1997).

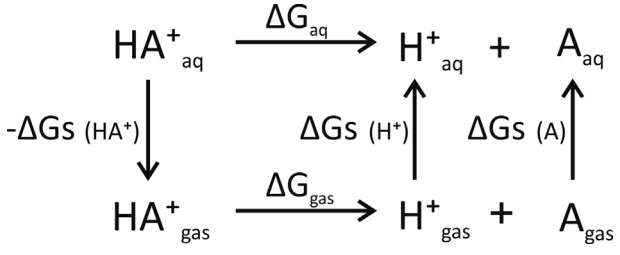

Fig. 1 Thermodynamic cycle used for pKa calculations. ΔG_{gas} – free energy of deprotonation in gas-phase; ΔG_s – solvation free energy; ΔG_{aq} – free energy of deprotonation in an aqueous solution.

3. Results and discussion

We studied the complexation of various biologically important divalent and trivalent metal cations with dopamine *o*-quinone. Possible complexes were further characterised using QTAIM analysis and quantum chemical reactivity indices, after which the effects of divalent and trivalent metal cations on pKa values, cyclization reaction mechanism, and activation free ener-

gies were determined. Finally, the effect of pH on activation free energies and reaction kinetics was investigated.

3.1. Binding affinities of metal cation-dopamine o-quinone complexes

For 1:1 complexes, the equilibriums between divalent (M^{2+}) and trivalent (M^{3+}) metal cations with neutral (DAQ) and protonated (DAQ^{+}) dopamine *o*-quinones are shown by the following equations respectively:

$$M^{2+} + DAQ = MDAQ^{2+} \quad (10)$$

$$M^{2+} + DAQ^{+} = MDAQ^{3+} \quad (11)$$

and

$$M^{3+} + DAQ = MDAQ^{3+} \quad (12)$$

$$M^{3+} + DAQ^{+} = MDAQ^{4+} \quad (13)$$

The stability constant values ($\log K_1$) are given as:

$$\log K_1 = \frac{-\Delta G}{2.303RT} \quad (14)$$

The binding free energies and stability constant values are shown in Table 1. All studied complexes between divalent and trivalent metal cations and dopamine *o*-quinone except complex with Mn^{2+} had negative binding free energies, suggesting that complexation of most studied metal cations and dopamine *o*-quinone is thermodynamically favourable. The complexation of Mn^{2+} with dopamine *o*-quinone is thermodynamically not favourable, which is also supported by experimental kinetic data where Mn^{2+} did not significantly affect the mechanism and kinetics of dopamine *o*-quinone cyclization (Lloyd, 1995). Moreover, the trivalent cations Al^{3+} and divalent cation Ni^{2+} had the largest biding affinities and stability constants, followed by Fe^{3+}, Pb^{2+}, Cu^{2+}, Co^{2+}, Fe^{2+}, Cd^{2+} and Zn^{2+}. The binding affinities of all studied metal cations complexed with protonated dopamine *o*-quinones were smaller than for neutral dopamine *o*-quinones, suggesting that the positively charged amino tail has an electron withdrawal effect, which is mediated by electron attracting behaviour of positive charge. In the study by Dalla Torre et al., a similar observation was noted for complexes of Al^{3+} and catecholamines. For Al^{3+} cation, it was also shown that in aqueous solution at physiological pH the formation of $Al(OH)_4^-$ is more favourable than complexation with catecholamines (Dalla Torre et al., 2019). However, since the free energy of hydroxide ion formation which is given by $k_B T ln(10)(15.7 - pH)$, where 15.7 is pKa of a water molecule (Bronsted, 1928), is very high at acidic pH, the formation of hydroxide ion becomes thermodynamically less favourable making the complexation with catecholamines more likely.

Our results also show that the stability constants of the complexes between divalent and trivalent metal cations and dopamine *o*-quinone are the highest for high spin, intermediate for intermediate spin and the lowest for low spin states (Table 1), suggesting that the low- and intermediate spin state complexes are thermodynamically less favourable. Accordingly, only high spin state complexes were investigated further.

3.2. Properties of metal–oxygen atom bonds in metal cation-dopamine o-quinone complexes

To characterise metal–oxygen atom bonds, the QTAIM analysis at BCPs was performed for each studied metal cation-dopamine *o*-quinone complex shown in Fig. 2. Each complex forms two metal–oxygen atom bonds, for which the topological parameters are reported in Table 2. The electron density (ρ(r)) at BCP is a measure of the strength of the bond. Metal–oxygen atom bonds involving divalent cations Fe^{2+} and Ni^{2+} had the largest ρ(r), followed by Cu^{2+}, Fe^{3+}, Al^{3+}, Co^{2+}, Zn^{2+}, Cd^{2+}, Pb^{2+} and Mn^{2+}. The Laplacian of the electron density ($\nabla 2\rho(r)$) at BCP characterizes a bond in terms of negative (covalent bond) or positive (electrostatic

Table 1 Binding energies (ΔG) and stability constants ($\log K_1$) for 1:1 complexes of divalent and trivalent metal cations with dopamine *o*-quinone (DAQ).

		DAQ with unprotonated amino group		DAQ with protonated amino group	
Complex	Spin state	ΔG (kcal mol^{-1})	$\log K_1$	ΔG (kcal mol^{-1})	$\log K_1$
Al^{3+}-DAQ	–	−46.61	34.15	−42.89	31.42
Mn^{2+}-DAQ	HS	3.57	−2.62	4.22	−3.09
	IS	27.91	−20.45	39.711	−29.09
	LS	89.53	−65.59	90.50	−66.30
Fe^{2+}-DAQ	HS	−8.22	6.02	−7.36	5.39
	LS	37.08	−27.17	59.86	−43.86
Fe^{3+}-DAQ	HS	−17.27	12.65	−12.15	8.90
	IS	−16.91	12.38	6.33	−4.64
	LS	15.28	−11.20	57.18	−41.89
Co^{2+}-DAQ	HS	−8.92	6.53	−6.43	4.71
	LS	23.31	−17.08	22.98	−16.83
Ni^{2+}-DAQ	HS	−37.74	27.65	−36.32	26.61
	LS	−8.48	6.21	−4.37	3.21
Cu^{2+}-DAQ	–	−10.87	7.96	−9.39	6.88
Zn^{2+}-DAQ	–	−3.12	2.29	−1.43	1.05
Cd^{2+}-DAQ	–	−3.81	2.79	−2.67	1.95
Pb^{2+}-DAQ	–	−12.76	9.35	−10.47	7.67

HS-high spin; IS-intermediate spin; LS-low spin; –not applicable.

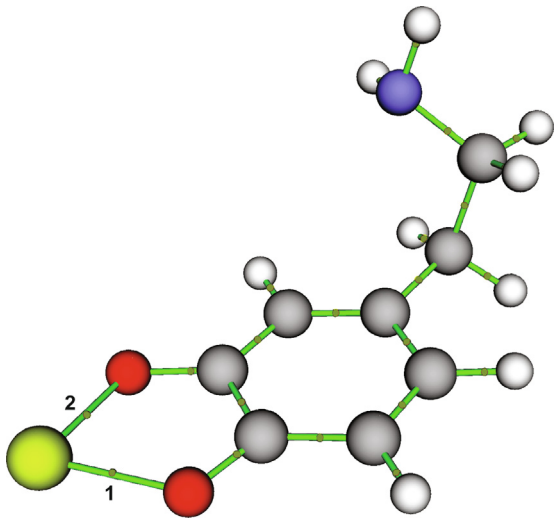

Fig. 2 Metal cation-dopamine *o*-quinone complex with unprotonated amino group with marked bond critical points. Carbon atoms are represented with grey, oxygen atoms with red, hydrogen atoms with white, nitrogen atoms with blue, and metal cation with yellow colour. Numbers 1 and 2 denote specific bond critical points which electronical density analyses are presented in Table 2.

interactions, hydrogen bond or van der Waals interactions) values, while the nature of the bond is denoted by the negative ratio of kinetic to potential energy density (–G(r)/V(r)) at BCP. The positive values of $\nabla^2\rho(r)$ and the values of -G(r)/V(r) near 1 (Table 2) indicate that the interactions between the oxygen atoms and metal cations are electrostatic and partially covalent (Crisponi and Nurchi, 2011; Grabowski, 2011). The bond ellipticity (ε) at the BCP, a derivative of the Hessian matrix of the electron density, demonstrated that the predominant character of the metal–oxygen atom bond is the σ-type character (Silva Lopez and R. de Lera, 2011). The heterogeneity in our results suggests that because of their dative nature, metal–oxygen atom bonds are mainly electrostatic with some degree of covalency (Gervasio et al., 2004). A similar finding was recently shown for Al-oxygen atom bonds in complexes of Al^{3+} and catecholamines and for metal–oxygen atom bonds in some other organometallic complexes such as Fe^{3+}-hydroxypyridinones (Dalla Torre et al., 2019; Kaviani et al., 2018).

3.3. Chemical reactivity of metal cation-dopamine o-quinone complexes

Chemical reactivity of metal cation-dopamine *o*-quinone complexes was assessed using frontier molecular orbital analysis and quantum chemistry reactivity indices such as HOMO-LUMO energy gap, electronic chemical hardness, electronic chemical potential, and electrophilicity index. The HOMO-LUMO energy gap ($\Delta E_{gap} = E_{LUMO} - E_{HOMO}$) correlates with the charge transfer interaction within the molecule (Aihara, 1999). Global chemical hardness η and electronic chemical potential μ describe the charge transfer within a system in the ground state and are calculated as:

$$\eta = \frac{E_{LUMO} - E_{HOMO}}{2} \tag{15}$$

and

$$\mu = \frac{E_{LUMO} + E_{HOMO}}{2}, \tag{16}$$

where more negative values of chemical potential suggest higher chemical reactivity. The global electrophilicity index ω

Table 2 Electron density (ρ(r)), Laplacian of electron density (∇2ρ(r)), negative ratio of kinetic energy density to the potential energy density (−G(r)/V(r)) and ellipticity of the electron density (ε) at bond critical points of metal–oxygen atom (M—O) bonds of metal cation-dopamine *o*-quinone (DAQ) complexes (Fig. 2). Results are presented in atomic units (a.u.).

		DAQ with unprotonated amino group				DAQ with protonated amino group			
Complex	Bond	ρ(r)	∇2ρ(r)	−G(r)/V(r)	ε	ρ(r)	∇2ρ(r)	−G(r)/V(r)	ε
Al^{3+}-DAQ	M—O_1	0.0672	0.268	0.860	0.053	0.0657	0.335	0.892	0.048
	M—O_2	0.0726	0.307	0.864	0.077	0.0707	0.395	0.889	0.068
Mn^{2+}-DAQ	M—O_1	0.0354	0.153	0.949	0.036	0.0375	0.164	0.945	0.031
	M—O_2	0.0477	0.215	0.920	0.013	0.0407	0.180	0.936	0.023
Fe^{2+}-DAQ	M—O_1	0.0916	0.425	0.855	0.201	0.0943	0.435	0.852	0.184
	M—O_2	0.0853	0.378	0.854	0.167	0.0865	0.381	0.852	0.156
Fe^{3+}-DAQ	M—O_1	0.0663	0.238	0.852	0.052	0.0675	0.242	0.850	0.053
	M—O_2	0.0849	0.324	0.834	0.014	0.0784	0.291	0.838	0.030
Co^{2+}-DAQ	M—O_1	0.0587	0.288	0.904	0.547	0.0708	0.357	0.888	0.540
	M—O_2	0.0617	0.302	0.898	0.545	0.0719	0.362	0.886	0.537
Ni^{2+}-DAQ	M—O_1	0.0851	0.426	0.861	0.033	0.0848	0.424	0.862	0.032
	M—O_2	0.0868	0.430	0.858	0.032	0.0849	0.422	0.860	0.031
Cu^{2+}-DAQ	M—O_1	0.0826	0.393	0.851	0.042	0.0766	0.362	0.856	0.062
	M—O_2	0.0770	0.356	0.854	0.039	0.0782	0.367	0.853	0.057
Zn^{2+}-DAQ	M—O_1	0.0563	0.282	0.953	0.020	0.0504	0.246	0.966	0.026
	M—O_2	0.0590	0.297	0.947	0.015	0.0591	0.301	0.949	0.018
Cd^{2+}-DAQ	M—O_1	0.0424	0.181	0.953	0.015	0.0421	0.180	0.955	0.016
	M—O_2	0.0511	0.227	0.940	0.008	0.0484	0.213	0.945	0.011
Pb^{2+}-DAQ	M—O_1	0.0434	0.145	0.927	0.023	0.0433	0.145	0.928	0.023
	M—O_2	0.0479	0.163	0.915	0.013	0.0451	0.152	0.923	0.018

on the other hand determines the favourable energy change when a chemical system becomes saturated by the addition of electrons and is calculated as (Parr et al., 1999):

$$\omega = \frac{\mu^2}{2\eta} \tag{17}$$

Results presented in Table 3 show that during a complex formation, the electronic hardness and electronic chemical potential decreased while electrophilicity increased, suggesting that metal cation-dopamine *o*-quinone complexes are more reactive than dopamine *o*-quinone. Moreover, dopamine *o*-quinone complexes with Ni^{2+}, Cu^{2+}, Al^{3+} and Pb^{2+} exhibited the highest chemical reactivity among the studied complexes.

3.4. The pKa values of metal cation-dopamine o-quinone complexes

Since the cost in terms of free energy for deprotonation of the amino group of dopamine *o*-quinone is necessary for the cyclization reaction to occur, we investigated the effect of complexation of metal cations and the dopamine *o*-quinone on its pKa values. The calculated pKa values of dopamine *o*-quinone and metal cation-dopamine *o*-quinone complexes are shown in Table 4. The complexation with metal cations causes a decrease of pKa values from 0.47 to 3.46. This suggests that the positive charge of metal cation electrostatically affects the protonated amino group of the dopamine *o*-quinone. Since the free energy differences of proton transfer from the ionizable group with a certain pKa value to bulk water with a certain pH bears the following relation $\Delta G = k_B T \ln(10)(pKa - pH)$, the complexation of dopamine *o*-quinone with metal cations thermodynamically favours the amino group deprotonation by decreasing the energy of proton transfer from the amino group to bulk water for 0.64–4.51 kcal mol^{-1} at any given pH value. Such influence of a charge on the pKa value of a nearby ionizable group has already been established in proteins (Pace et al., 2009). The apparent decrease in pKa value of dopamine amino group in the presence of Fe^{3+} and Cu^{2+} ions was also indirectly observed by Salomäki et al. while studying the dopamine autoxidation rates at different pH values with and without the presence of the forementioned metal cations. It was also theoretically predicted that the pKa value of the dopamine amino group would decrease by approximately 0.45 per unit of positive charge (Salomäki et al., 2018).

Calculations of pKa values are very demanding and can serve as one of the strictest tests for the efficiency of various solvation models (Kavcic et al., 2021; Repič et al., 2014; Warshel, 1981). Our results show that the calculated pKa value of dopamine *o*-quinone ($pKa^{calc} = 8.73$) is in good agreement with the experimental pKa value of dopamine ($pKa^{exp} = 8.86$) (Berfield et al., 1999) showing that the SMD reaction field solvation model with M06/Def2-TZVPP level of theory is sufficiently accurate. Note that because of the topological proximity (six bonds away) of the closest carbonyl group from the amino group, the pKa value of the dopamine amino group was applied as an approximation on account of lack of the

Table 3 Chemical reactivity of metal cation-dopamine *o*-quinone (DAQ) complexes determined by HOMOLUMO energy gap (ΔE_{gap}), chemical hardness (η), electronic chemical potential (μ) and electrophilicity index (ω). Results are presented in atomic units (a. u.).

	DAQ with unprotonated amino group				DAQ with protonated amino group			
Complex	ΔE_{gap}	η	μ	ω	ΔE_{gap}	η	μ	ω
DAQ	0.1332	0.0666	−0.1915	0.2754	0.1471	0.0735	−0.2036	0.2818
Al^{3+}-DAQ	0.0900	0.0450	−0.2215	0.5449	0.1285	0.0642	−0.2472	0.4757
Mn^{2+}-DAQ	0.0942	0.0471	−0.2164	0.4975	0.1131	0.0566	−0.2192	0.4248
Fe^{2+}-DAQ	0.1184	0.0592	−0.2018	0.3441	0.1293	0.0647	−0.2210	0.3776
Fe^{3+}-DAQ	0.0917	0.0458	−0.2224	0.5395	0.1296	0.0648	−0.2480	0.4745
Co^{2+}-DAQ	0.1091	0.0546	−0.2087	0.3991	0.1342	0.0671	−0.2321	0.4014
Ni^{2+}-DAQ	0.0831	0.0416	−0.2234	0.6006	0.1311	0.0655	−0.2398	0.4387
Cu^{2+}-DAQ	0.0872	0.0436	−0.2209	0.5594	0.1184	0.0592	−0.2433	0.5002
Zn^{2+}-DAQ	0.0915	0.0458	−0.2183	0.5207	0.1345	0.0672	−0.2323	0.4013
Cd^{2+}-DAQ	0.1148	0.0574	−0.2054	0.3674	0.1329	0.0664	−0.2347	0.4147
Pb^{2+}-DAQ	0.0917	0.0459	−0.2216	0.5356	0.1343	0.0672	−0.2298	0.3930

Table 4 Partial charge of metal cations, amino group pKa values and changes of free energy of amino group deprotonation (ΔΔG) of metal cation-dopamine *o*-quinone complexes compared to dopamine *o*-quinone (DAQ).

Complex	DAQ	Al^{3+}-DAQ	Mn^{2+}-DAQ	Fe^{2+}-DAQ	Fe^{3+}-DAQ	Co^{2+}-DAQ	Ni^{2+}-DAQ	Cu^{2+}-DAQ	Zn^{2+}-DAQ	Cd^{2+}-DAQ	Pb^{2+}-DAQ
Partial charge of metal cation	–	2.29	1.91	2.27	2.58	1.82	1.67	1.72	1.83	1.85	1.65
pKa	8.73	6.00	8.26	8.09	5.41	6.91	7.69	7.65	7.5	7.9	7.05
ΔΔG (kcal mol^{-1})	–	−3.70	−0.64	−0.87	−4.51	−2.47	−1.41	−1.47	−1.67	−1.13	−2.28

– not applicable.

exact experimental pKa value for dopamine *o*-quinone amino group. The latter is not experimentally accessible due to the very fast cyclization rate at alkaline pH and the instability of dopamine *o*-quinone.

3.5. Mechanism and pH dependence of metal cation-dopamine o-quinone cyclization

Our results show that in contrast to dopamine *o*-quinone cyclization in aqueous solution where a hydroxide anion must first extract a proton from unprotonated amino group (Fig. 3A) (Umek et al., 2018), a cyclization of 1:1 metal cation-dopamine *o*-quinone with unprotonated amino group can proceed spontaneously as suggested by negative reaction free energies (Table 5, Fig. 3b). For all the studied complexes a transition state was searched for, and the intrinsic activation free energy ($\Delta G_i^{\neq}$) calculated (Table 5), which was the lowest and basically barrierless for dopamine o-quinone complexes with Al^{3+} and Fe^{3+} cations. Note that at physiological pH values, complete activation free energy ($\Delta G^{\neq}$) that would be comparable to the experimental values also includes the energy of amino group deprotonation. Therefore, the complete activation free energy for cation-dopamine *o*-quinone cyclization is given by:

$$\Delta G^{\neq} = \Delta G_i^{\neq} + k_B T \ln(10)(pKa - pH) \tag{18}$$

Inserting the latter into the transition state equation.

$$k_{rate} = \frac{k_B T}{h} e^{-\left(\frac{\Delta G^{\neq}}{k_B T}\right)} \tag{19}$$

gives pH dependences of reaction rate,

$$k_{rate}(pH) = \frac{k_B T}{h} e^{-\left(\frac{\Delta G_i^{\neq} + k_B T \ln(10)(pKa - pH)}{k_B T}\right)} \tag{20}$$

from which the following functional form can be derived:

$$k_{rate}(pH) = 10^{-(c - pH)} \tag{21}$$

The latter is qualitatively fully consistent with experimental pH dependence of dopamine, adrenaline, and noradrenaline autoxidation rate in aqueous solution in the presence of Fe^{3+} ions (El-Ayaan et al., 1998, 1997; Linert et al., 1993). Please note that since bulk water is a proton rich environment, the rearrangement of protons after the cyclization step was not investigated because the proton diffusion rate in an aqueous solution is very fast and does not represent a rate-limiting step (Umek et al., 2018).

Table 5 Reaction and activation free energies for cyclization reaction of dopamine *o*-quinone (DAQ) initiated by an attack of hydroxide ion (OH^-) and for spontaneous cyclization reactions of metal cation-dopamine *o*-quinone complexes in aqueous solution (Fig. 3).

Complex	Reaction free energy (kcal mol^{-1})	Activation free energy (kcal mol^{-1})
DAQ + OH^-	−23.72	10.95
Al^{3+}-DAQ	−29.72	1.11
Mn^{2+}-DAQ	−8.91	8.98
Fe^{2+}-DAQ	−7.78	11.92
Fe^{3+}-DAQ	−33.34	1.68
Co^{2+}-DAQ	−12.61	9.03
Ni^{2+}-DAQ	−23.63	3.28
Cu^{2+}-DAQ	−20.10	4.58
Zn^{2+}-DAQ	−13.15	7.56
Cd^{2+}-DAQ	−10.04	8.71
Pb^{2+}-DAQ	−17.82	5.82

Results therefore show that most of the studied metal cations can significantly increase the dopamine *o*-quinone cyclization rate in aqueous solution, first, by enabling the cyclization to proceed spontaneously without the attack of the unprotonated amino group by hydroxide ion; second by, decreasing the intrinsic activation energy; and third, by decreasing the free energy of protonated amino group deprotonation. It also relatively decreases the protective effect of acidic pH on dopamine autoxidation. This could be biologically important in the aspect of neurodegeneration, since with age and in various pathological conditions, different metals can accumulate in the various tissues, including the brain, and the mechanisms that counteract metal neurotoxicity could become less efficient (Paris and Segura-Aguilar, 2011).

At this point, it is worth stressing that synaptic vesicles, cytosol, and extracellular fluid are very complex environments with many molecules such as citrate that could act as endogenous chelators that could bind metal cations and ameliorate their toxic effect (Chua et al., 2010; Dalla Torre et al., 2019). Moreover, Jiang et al. showed that stabilization of Fe^{3+} by ATP molecule that is abundant in the neurons and also acts as co-transmitter could significantly decrease the ability of Fe^{3+} to catalyse dopamine autoxidation (Jiang et al., 2013). Furthermore, it was also proposed that complexes of catecholamines, Fe^{3+}, and ATP are produced in neurons or synaptic clefts as a protective measure against oxidative stress

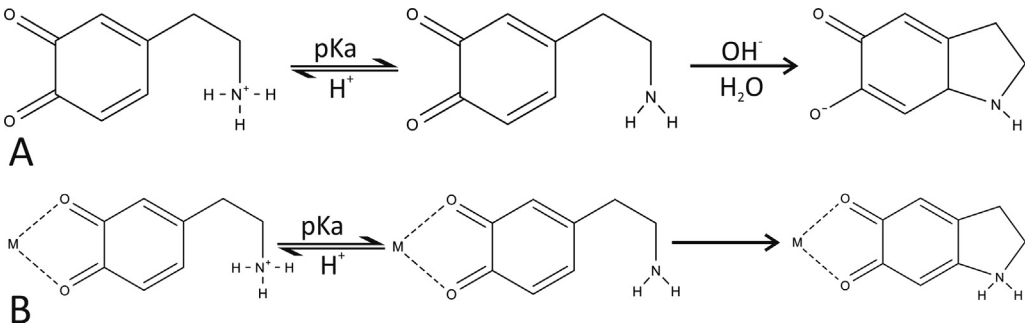

Fig. 3 Dopamine *o*-quinone cyclization reaction (A) and metal cation-dopamine *o*-quinone complex cyclization reaction (B) in aqueous solution.

(Kou et al., 2019). Accordingly, further experimental studies examining the role of metal cations in catecholaminergic neurodegeneration are warranted.

The implicit SMD solvation model was used to represent the aqueous solution, therefore, the hydrogen bonds between studied complexes and water molecules were not explicitly considered. Since hydrogen bonds can have a crucial role for the structure and interactions of biomolecules, they could influence the studied reactions (Benmalti et al., 2009; Flakus et al., 2012; Rekik et al., 2015). However, the quantitative theoretical treatment of hydrogen-bonded systems is very demanding, and even the most advanced theories are sometimes not able to sufficiently describe them (Ghalla et al., 2010; Rekik, 2014; Rekik et al., 2016). Therefore, it remains a challenge to address these reactions on multiscale QM/MM level with explicit solvation model.

4. Conclusions

Using the quantum chemical methods, we investigated the effects of various divalent and trivalent metal cations on the cyclization step of dopamine autoxidation in an aqueous solution. We showed that except for Mn^{2+}, the complexation of other studied metal cations (Al^{3+}, Fe^{3+}, Fe^{2+}, Co^{2+}, Ni^{2+}, Cu^{2+}, Zn^{2+}, Cd^{2+}, Pb^{2+}) with dopamine *o*-quinone, which is the form entering the cyclization reaction, is thermodynamically favourable, that the bonds between metal cations and dopamine *o*-quinone are mainly of electrostatic nature, and that these complexes have higher chemical reactivity than dopamine *o*-quinone itself. Furthermore, we showed that metal cations could significantly increase the dopamine *o*-quinone cyclization rate in aqueous solution: (a) by enabling the cyclization to proceed spontaneously without the attack of the unprotonated amino group by hydroxide ion, (b) by decreasing the intrinsic activation energy, and (c) by decreasing the free energy of protonated amino group deprotonation, which also relatively decreases the protective effect of acidic pH on dopamine autoxidation. The results are fully consistent with experimental data and provide a deeper understanding of the effects of metal cations on the rate-determining step of dopamine autoxidation at physiologic pH values. They support the notion that biologically important divalent and trivalent metal cations could increase the rate of dopamine autoxidation in cellular compartments with neutral pH, such as cytosol end extracellular fluid, and compartments with acidic pH, such as synaptic vesicle. Thus, they could increase the oxidative stress and aminochrome production which can both lead to neurodegeneration and dopaminergic cell loss. It remains a challenge for the future to build a macroscopic model of catecholaminergic neurodegeneration under different pathologic conditions including heavy metal toxicity (Pregeljc et al., 2020).

Declaration of Competing Interest

The authors declare that they have no known competing financial interests or personal relationships that could have appeared to influence the work reported in this paper.

Acknowledgments

The author would like to thank professor Janez Mavri for critical review of the manuscript; Dr. Robert Vianello for many stimulating discussions; Damjan Tkalec for technical support; Nejc Petrišič for help with graphics; Chiedozie Kenneth Ugwoke for manuscript proofreading; and the National Institute of Chemistry for CPU time. This work was supported by the Slovenian Research Agency (grant number P3-0043).

References

Aihara, J.I., 1999. Reduced HOMO-LUMO gap as an index of kinetic stability for polycyclic aromatic hydrocarbons. J. Phys. Chem. A 103, 7487–7495. https://doi.org/10.1021/jp990092i.

Bacil, R.P., Chen, L., Serrano, S.H.P., Compton, R.G., 2020. Dopamine oxidation at gold electrodes: Mechanism and kinetics near neutral pH. PCCP 22, 607–614. https://doi.org/10.1039/c9cp05527d.

Bader, R.F.W., 1991. A Quantum Theory of Molecular Structure and Its Applications. Chem. Rev. 91, 893–928. https://doi.org/10.1021/cr00005a013.

Baez, S., Linderson, Y., Segura-Aguilar, J., 1994. Superoxide dismutase and catalase prevent the formation of reactive oxygen species during reduction of cyclized dopa ortho-quinone by DT-diaphorase. Chem. Biol. Interact. 93, 103–116. https://doi.org/10.1016/0009-2797(94)90090-6.

Benmalti, M.E.A., Krallafa, A., Rekik, N., Belhakem, M., 2009. Theoretical study of the νO-H IR spectra for the hydrogen bond dimers from the polarized spectra of glutaric and 1-naphthoic acid crystals: Fermi resonances effects. Spectrochim. Acta – Part A Mol. Biomol. Spectrosc. 74, 58–66. https://doi.org/10.1016/j.saa.2009.05.005.

Berfield, J.L., Wang, L.C., Reith, M.E.A., 1999. Which form of dopamine is the substrate for the human dopamine transporter: The cationic or the uncharged species? J. Biol. Chem. 274, 4876–4882. https://doi.org/10.1074/jbc.274.8.4876.

Bindoli, A., Scutari, G., Rigobello, M.P., 1999. The role of adrenochrome in stimulating the oxidation of catecholamines. Neurotox. Res. 1, 71–80.

Branca, J.J.V., Morucci, G., Pacini, A., 2018. Cadmium-induced neurotoxicity: Still much ado. Neural Regen. Res. 13, 1879–1882. https://doi.org/10.4103/1673-5374.239434.

Bronsted, J.N., 1928. Acid and Basic Catalysis. Chem. Rev. 5, 231–338. https://doi.org/10.1021/cr60019a001.

Canfield, R.L., Henderson, C.R., Cory-Slechta, D.A., Cox, C., Jusko, T.A., Lanphear, B.P., 2003. Intellectual Impairment in Children with Blood Lead Concentrations below 10 μg per Deciliter. N. Engl. J. Med. 348, 1517–1526. https://doi.org/10.1056/nejmoa022848.

Cassagnes, L.-E.-E., Chhour, M., Pério, P., Sudor, J., Gayon, R., Ferry, G., Boutin, J.A., Nepveu, F., Reybier, K., 2018. Oxidative stress and neurodegeneration: The possible contribution of quinone reductase 2. Free Radic. Biol. Med. 120, 56–61. https://doi.org/10.1016/j.freeradbiomed.2018.03.002.

Catalani, S., Rizzetti, M.C., Padovani, A., Apostoli, P., 2012. Neurotoxicity of cobalt. Hum. Exp. Toxicol. 31, 421–437. https://doi.org/10.1177/0960327111414280.

Chaudhry, F.A., Edwards, R.H., Fonnum, F., 2008. Vesicular neurotransmitter transporters as targets for endogenous and exogenous toxic substances. Annu. Rev. Pharmacol. Toxicol. 48, 277–301. https://doi.org/10.1146/annurev.pharmtox.46.120604.141146.

Chua, J.J.E., Kindler, S., Boyken, J., Jahn, R., 2010. The architecture of an excitatory synapse. J. Cell Sci. 123, 819–823. https://doi.org/10.1242/jcs.052696.

Crisponi, G., Nurchi, V.M., 2011. Thermodynamic remarks on chelating ligands for aluminium related diseases. J. Inorg. Biochem. 105, 1518–1522. https://doi.org/10.1016/j.jinorgbio.2011.07.004.

Dalla Torre, G., Mujika, J.I., Lachowicz, J.I., Ramos, M.J., Lopez, X., 2019. The interaction of aluminum with catecholamine-based neurotransmitters: Can the formation of these species be considered a potential risk factor for neurodegenerative diseases? Dalt. Trans. 48, 6003–6018. https://doi.org/10.1039/c8dt04216k.

Du, J., Reznikov, L.R., Price, M.P., Zha, X.M., Lu, Y., Moninger, T.O., Wemmie, J.A., Welsha, M.J., 2014. Protons are a neurotransmitter that regulates synaptic plasticity in the lateral amygdala.

Proc. Natl. Acad. Sci. U. S. A. 111, 8961–8966. https://doi.org/10.1073/pnas.1407018111.

El-Ayaan, U., Herlinger, E., Jameson, R.F., Linert, W., 1997. Anaerobic oxidation of dopamine by iron(III). J. Chem. Soc. – Dalt. Trans. 2813–2818. https://doi.org/10.1039/a701054k.

El-Ayaan, U., Jameson, R.F., Linert, W., 1998. A kinetic study of the reaction between noradrenaline and iron(III): An example of parallel inner- and outer-sphere electron transfer. J. Chem. Soc. – Dalt. Trans. 1315–1319. https://doi.org/10.1039/a708639c.

Flakus, H.T., Rekik, N., Jarczyk, A., 2012. Polarized IR spectra of the hydrogen bond in 2-thiopheneacetic acid and 2-thiopheneacrylic acid crystals: H/D isotopic and temperature effects. J. Phys. Chem. A 116, 2117–2130. https://doi.org/10.1021/jp210950n.

Frisch, M.J., Trucks, G.W., Schlegel, H.E., Scuseria, G.E., Robb, M. A., Cheeseman, J.R., Scalmani, G., Barone, V., Petersson, G.A.O. F., Foresman, J.B., Fox, J.D., 2016. Gaussian 16. Gaussian, Inc., Wallingford CT.

Gergely, A., Kiss, T., Deák, G., Sóvágó, I., 1981. Complexes of 3,4-dihydroxyphenyl derivatives IV. Equilibrium studies on some transition metal complexes formed with adrenaline and noradrenaline. Inorganica Chim. Acta 56, 35–40. https://doi.org/10.1016/S0020-1693(00)88544-8.

Gervasio, G., Bianchi, R., Marabello, D., 2004. About the topological classification of the metal-metal bond. Chem. Phys. Lett. 387, 481–484. https://doi.org/10.1016/j.cplett.2004.02.043.

Ghalla, H., Rekik, N., Michta, A., Oujia, B., Flakus, H.T., 2010. Theoretical modeling of infrared spectra of the hydrogen and deuterium bond in aspirin crystal. Spectrochim. Acta – Part A Mol Biomol. Spectrosc. 75, 37–47. https://doi.org/10.1016/j.saa.2009.09.029.

Grabowski, S.J., 2011. What is the covalency of hydrogen bonding? Chem. Rev. 111, 2597–2625. https://doi.org/10.1021/cr800346f.

Grgas-Kužnar, B., Simeon, V., Weber, O.A., 1974. Complexes of adrenaline and related compounds with Ni2+, Cu2+, Zn2+, Cd2+ and Pb2+. J. Inorg. Nucl. Chem. 36, 2151–2154. https://doi.org/10.1016/0022-1902(74)80741-4.

Harrison, W.H., Whisler, W.W., Hill, B.J., 1968. Catecholamine oxidation and ionization properties indicated from the H+ release, tritium exchange, and spectral changes which occur during ferricyanide oxidation. Biochemistry 7, 3089–3094.

Herrera, A., Muñoz, P., Steinbusch, H.W.M., Segura-Aguilar, J., 2017. Are Dopamine Oxidation Metabolites Involved in the Loss of Dopaminergic Neurons in the Nigrostriatal System in Parkinson's Disease? ACS Chem. Neurosci. 8, 702–711. https://doi.org/10.1021/acschemneuro.7b00034.

Ho, J., Coote, M.L., 2009. A universal approach for continuum solvent pKa calculations: Are we there yet? Theor. Chem. Acc. 125, 3–21. https://doi.org/10.1007/s00214-009-0667-0.

Jameson, R.F., Neillie, W.F.S., 1965. Complexes formed by adrenaline and related compounds with transition-metal ions-II complexes with copper(II). J. Inorg. Nucl. Chem. 27, 2623–2634. https://doi.org/10.1016/0022-1902(65)80166-X.

Jameson, R.F., Neillie, W.F.S., 1966. Complexes formed by adrenaline and related compounds with transition-metal ions-III. The stabilities of some first-row transition-metal complexes. J. Inorg. Nucl. Chem. 28, 2667–2675. https://doi.org/10.1016/0022-1902(66)80392-5.

Jiang, D., Shi, S., Zhang, L., Liu, L., Ding, B., Zhao, B., Yagnik, G., Zhou, F., 2013. Inhibition of the Fe(III)-catalyzed dopamine oxidation by ATP and its relevance to oxidative stress in Parkinson's disease. ACS Chem. Neurosci. 4, 1305–1313. https://doi.org/10.1021/cn400105d.

Kavcic, H., Umek, N., Pregeljc, D., Vintar, N., Mavri, J., 2021. Local Anesthetics Transfer Across the Membrane: Reproducing Octanol-Water Partition Coefficients by Solvent Reaction Field Methods. Acta Chim. Slov., 68 https://doiorg/10.17344/acsi.2020.6513.

Kaviani, S., Izadyar, M., Housaindokht, M.R., 2018. DFT investigation on the selective complexation of Fe3+ and Al3+ with hydroxypyridinones used for treatment of the aluminium and iron overload diseases. J. Mol. Graph. Model. 80, 182–189. https://doi.org/10.1016/j.jmgm.2018.01.003.

Khan, Y.S., Gutiérrez-De-Terán, H., Åqvist, J., 2018. Molecular Mechanisms in the Selectivity of Nonsteroidal Anti-Inflammatory Drugs. Biochemistry 57, 1236–1248. https://doi.org/10.1021/acs.biochem.7b01019.

Kou, L., Duan, Y., Wang, P., Fu, Y., Darabedian, N., He, Y., Jiang, D., Chen, D., Xiang, J., Liu, G., Zhou, F., 2019. Norepinephrine-Fe(III)-ATP Ternary Complex and Its Relevance to Parkinson's Disease. ACS Chem. Neurosci. 10, 2777–2785. https://doi.org/10.1021/acschemneuro.9b00009.

Kržan, M., Keuschler, J., Mavri, J., Vianello, R., 2020. Relevance of Hydrogen Bonds for the Histamine H2 Receptor-Ligand Interactions: A Lesson from Deuteration. Biomolecules 10, 2. https://doi.org/10.3390/biom10020196.

Lamtai, M., Chaibat, J., Ouakki, S., Zghari, O., Mesfioui, A., El Hessni, A., Rifi, E.H., Marmouzi, I., Essamri, A., Ouichou, A., 2018. Effect of chronic administration of nickel on affective and cognitive behavior in male and female rats: Possible implication of oxidative stress pathway. Brain Sci. 8. https://doi.org/10.3390/brainsci8080141.

Lin, C., Chen, L., Tanner, E.E.L., Compton, R.G., 2017. Electroanalytical study of dopamine oxidation on carbon electrodes: From the macro- to the micro-scale. PCCP 20, 148–157. https://doi.org/10.1039/c7cp07450f.

Linert, W., Herlinger, E., Jameson, R.F., 1993. A kinetic study of the anaerobic reactions between adrenaline and iron(III). J. Chem. Soc. Perkin Trans. 2, 2435–2439. https://doi.org/10.1039/p29930002435.

Liptak, M.D., Gross, K.C., Seybold, P.G., Feldgus, S., Shields, G.C., 2002. Absolute pKa determinations for substituted phenols. J. Am. Chem. Soc. 124, 6421–6427. https://doi.org/10.1021/ja012474j.

Lloyd, R.V., 1995. Mechanism of the manganese-catalyzed autoxidation of dopamine. Chem. Res. Toxicol. 8, 111–116.

Lu, T., Chen, F., 2012. Multiwfn: A multifunctional wavefunction analyzer. J. Comput. Chem. 33, 580–592. https://doi.org/10.1002/jcc.22885.

Mani, M., Ryan, T.A., 2009. Live imaging of synaptic vesicle release and retrieval in dopaminergic neurons. Front. Neural Circuits 3, 3. https://doi.org/10.3389/neuro.04.003.2009.

Marenich, A.V., Cramer, C.J., Truhlar, D.G., 2009. Universal solvation model based on solute electron density and on a continuum model of the solvent defined by the bulk dielectric constant and atomic surface tensions. J. Phys. Chem. B 113, 6378–6396. https://doi.org/10.1021/jp810292n.

Martin, R.B., 1994. Aluminum: A Neurotoxic Product of Acid Rain. Acc. Chem. Res. 27, 204–210. https://doi.org/10.1021/ar00043a004.

Martorana, A., Koch, G., 2014. Is dopamine involved in Alzheimer's disease? Front. Aging Neurosci. 6, 252. https://doi.org/10.3389/fnagi.2014.00252.

Morris, D.R., Levenson, C.W., 2017. Neurotoxicity of Zinc. Adv. Neurobiol. 18, 303–312. https://doi.org/10.1007/978-3-319-60189-2_15.

Ortega, R., Cloetens, P., Devès, G., Carmona, A., Bohic, S., 2007. Iron storage within dopamine neurovesicles revealed by chemical nano-imaging. PLoS ONE 2. https://doi.org/10.1371/journal.pone.0000925.

Pace, C.N., Grimsley, G.R., Scholtz, J.M., 2009. Protein ionizable groups: pK values and their contribution to protein stability and solubility. J. Biol. Chem. 284, 13285–13289. https://doi.org/10.1074/jbc.R800080200.

Paris, I., Perez-Pastene, C., Cardenas, S., Iturriaga-Vasquez, P., Iturra, P., Muñoz, P., Couve, E., Caviedes, P., Segura-Aguilar, J., 2010. Aminochrome induces disruption of actin, alpha-, and beta-tubulin cytoskeleton networks in substantia-nigra-derived cell line. Neurotox. Res. 18, 82–92. https://doi.org/10.1007/s12640-009-9148-4.

Paris, I., Segura-Aguilar, J., 2011. The role of metal ions in dopaminergic neuron degeneration in Parkinsonism and Parkin-

son's disease. Monatsh. Chem. 142, 365–374. https://doi.org/10.1007/s00706-011-0478-6.

Parr, R.G., Szentpály, L.V., Liu, S., 1999. Electrophilicity index. J. Am. Chem. Soc. 121, 1922–1924. https://doi.org/10.1021/ja983494x.

Pavlin, M., Repič, M., Vianello, R., Mavri, J., 2016. The Chemistry of Neurodegeneration: Kinetic Data and Their Implications. Mol. Neurobiol. 53, 3400–3415. https://doi.org/10.1007/s12035-015-9284-1.

Perdan-Pirkmajer, K., Mavri, J., Krŝan, M., 2010. Histamine (re) uptake by astrocytes: An experimental and computational study. J. Mol. Model. 16, 1151–1158. https://doi.org/10.1007/s00894-009-0624-9.

Piggott, M.A., Marshall, E.F., Thomas, N., Lloyd, S., Court, J.A., Jaros, E., Burn, D., Johnson, M., Perry, R.H., McKeith, I.G., Ballard, C., Perry, E.K., 1999. Striatal dopaminergic markers in dementia with Lewy bodies, Alzheimer's and Parkinson's diseases: rostrocaudal distribution. Brain 122, 1449–1468. https://doi.org/10.1093/brain/122.8.1449.

Pregeljc, D., Teodorescu-Perijoc, D., Vianello, R., Umek, N., Mavri, J., 2020. How Important Is the Use of Cocaine and Amphetamines in the Development of Parkinson Disease? A Computational Study. Neurotox. Res. 37, 724–731. https://doi.org/10.1007/s12640-019-00149-0.

Rappé, A.K., Casewit, C.J., Colwell, K.S., Goddard, W.A., Skiff, W. M., 1992. UFF, a Full Periodic Table Force Field for Molecular Mechanics and Molecular Dynamics Simulations. J. Am. Chem. Soc. 114, 10024–10035. https://doi.org/10.1021/ja00051a040.

Rekik, N., 2014. Toward accurate prediction of potential energy surfaces and the spectral density of hydrogen bonded systems. Phys. B Condens. Matter 436, 164–176. https://doi.org/10.1016/j.physb.2013.12.003.

Rekik, N., Flakus, H.T., Jarczyk-Jędryka, A., Abdulaziz Al-Agel, F., Daouahi, M., Jones, P.G., Kusz, J., Nowak, M., 2015. Elucidating the Davydov-coupling mechanism in hydrogen bond dimers: Experimental and theoretical investigation of the polarized IR spectra of 3-thiopheneacetic and 3-thiopheneacrylic acid crystals. J. Phys. Chem. Solids 77, 68–84. https://doi.org/10.1016/j.jpcs.2014.10.008.

Rekik, N., Al-Agel, F.A., Flakus, H.T., 2016. Davydov coupling as a factor influencing the H-bond IR signature: Computational study of the IR spectra of 3-thiopheneacrylic acid crystal. Chem. Phys. Lett. 647, 107–113. https://doi.org/10.1016/j.cplett.2016.01.042.

Repič, M., Purg, M., Vianello, R., Mavri, J., 2014. Examining electrostatic preorganization in monoamine oxidases A and B by structural comparison and pKa calculations. J. Phys. Chem. B 118, 4326–4332. https://doi.org/10.1021/jp500795p.

Sadiq, S., Ghazala, Z., Chowdhury, A., Büsselberg, D., 2012. Metal toxicity at the synapse: Presynaptic, postsynaptic, and long-term effects. J. Toxicol. 2012, 132671. https://doi.org/10.1155/2012/132671.

Salomäki, M.O., Marttila, L., Kivelä, H., Ouvinen, T., Lukkari, J.O., 2018. Effect of pH and Oxidant on the First Steps of Polydopamine Formation: A Thermodynamic Approach. J. Phys. Chem. B 122, 6314–6327. https://doi.org/10.1021/acs.jpcb.8b02304.

Schaftenaar, G., Noordik, J.H., 2000. Molden: a pre- and post-processing program for molecular and electronic structures. J. Comput. Aided Mol. Des. 14, 123–134.

Schindler, S., Bechtold, T., 2019. Mechanistic insights into the electrochemical oxidation of dopamine by cyclic voltammetry. J. Electroanal. Chem. 836, 94–101. https://doi.org/10.1016/j.jelechem.2019.01.069.

Segura-Aguilar, J., 2019. On the Role of Aminochrome in Mitochondrial Dysfunction and Endoplasmic Reticulum Stress in Parkinson's Disease. Front. Neurosci. 13, 271. https://doi.org/10.3389/fnins.2019.00271.

Segura-Aguilar, J., Metodiewa, D., Welch, C.J., 1998. Metabolic activation of dopamine o-quinones to o-semiquinones by NADPH cytochrome P450 reductase may play an important role in oxidative stress and apoptotic effects. BBA 1381, 1–6.

Sham, Y.Y., Chu, Z.T., Warshel, A., 1997. Consistent calculations of pKa's of ionizable residues in proteins: Semi-microscopic and microscopic approaches. J. Phys. Chem. B 101, 4458–4472. https://doi.org/10.1021/jp963412w.

Silva Lopez, C., de Lera, R.A., 2011. Bond Ellipticity as a Measure of Electron Delocalization in Structure and Reactivity. Curr. Org. Chem. 15, 3576–3593. https://doi.org/10.2174/138527211797636228.

Sun, Y., Pham, A.N., Hare, D.J., Waite, T.D., 2018. Kinetic modeling of pH-dependent oxidation of dopamine by iron and its relevance to Parkinson's disease. Front. Neurosci. 12, 859. https://doi.org/10.3389/fnins.2018.00859.

Umek, N., 2020. Cyclization step of noradrenaline and adrenaline autoxidation: a quantum chemical study. RSC Adv. 10, 16650–16658. https://doi.org/10.1039/d0ra02713h.

Umek, N., Gersak, B., Vintar, N., Sostaric, M., Mavri, J., 2018. Dopamine Autoxidation is Controlled by Acidic pH. Front. Mol. Neurosci. 11, 467. https://doi.org/10.3389/FNMOL.2018.00467.

Wang, X., Cheng, D., Jiang, W., Ma, Y., 2018. Mechanisms underlying aluminum neurotoxicity related to 14–3-3ζ protein. Toxicol. Sci. 163, 45–56. https://doi.org/10.1093/toxsci/kfy021.

Warshel, A., 1981. Calculations of enzymatic reactions: calculations of pKa, proton transfer reactions, and general acid catalysis reactions in enzymes. Biochemistry 20, 3167–3177.

Weigend, F., Ahlrichs, R., 2005. Balanced basis sets of split valence, triple zeta valence and quadruple zeta valence quality for H to Rn: Design and assessment of accuracy. PCCP 7, 3297–3305. https://doi.org/10.1039/b508541a.

Zhao, Y., Truhlar, D.G., 2008. The M06 suite of density functionals for main group thermochemistry, thermochemical kinetics, noncovalent interactions, excited states, and transition elements: Two new functionals and systematic testing of four M06-class functionals and 12 other function. Theor. Chem. Acc. 120, 215–241. https://doi.org/10.1007/s00214-007-0310-x.